ARTICLE

BIOTECHNOLOGY and BIOENGINEERING

Enhanced Secretion of Recombinant Proteins Via Signal Recognition Particle (SRP)-Dependent Secretion Pathway by Deletion of *rrsE* in *Escherichia coli*

Yong Jae Lee,[1] Roojin Lee,[1] Se Hwa Lee,[1] Sung Sun Yim,[1] Ki Jun Jeong[1,2]

[1]Department of Chemical and Biomolecular Engineering (BK21 Program), KAIST, 291 Daehak-ro, Yuseong-gu, Daejeon 34141, Republic of Korea; telephone: +82-42-350-3934; fax: +82-42-350-3910; e-mail: kjjeong@kaist.ac.kr

[2]KAIST Institute for the BioCentury, Yuseong-gu, Daejeon, Republic of Korea

ABSTRACT: Although signal recognition particle (SRP)-dependent secretion pathway, which is characterized by co-translational translocation, helps prevent cytoplasmic aggregation of proteins before secretion, its limited capacity for the protein secretion is a major hurdle for utilizing the pathway as an attractive route for secretory production of recombinant proteins. Therefore, we developed an *Escherichia coli* mutant, whose efficiency of secretion via the SRP pathway was dramatically increased. First, we developed a novel FACS-based screening system by combining a periplasmic display system (PECS) and direct fluorescent labeling with the organoarsenic compound, FlAsH-EDT_2. With this screening system, transposon-insertion library of *E. coli* was screened, and then we isolated mutants which exhibited higher protein production through the SRP pathway than the parental strain. From the genetic analysis, we found that all isolated mutants had the same mutation—disruption of the 16S rRNA gene (*rrsE*). The positive effect of *rrsE* deficiency on protein secretion via the SRP pathway was successfully demonstrated using various model proteins including endogenous SRP-dependent proteins, antibodies, and G protein-coupled receptor. For the large-scale production of IgG and GPCR, we performed fed-batch cultivation with the *rrsE*-deficient mutant, and very high yields of IgG (0.4 g/L) and GPCR (1.4 g/L) were obtained.

Biotechnol. Bioeng. 2016;113: 2453–2461.

KEYWORDS: *Escherichia coli*; SRP-dependent secretion; FACS; 16S ribosomal RNA; G protein-coupled receptor (GPCR)

Introduction

For a long time, *Escherichia coli* has been a workhorse for the production of various recombinant proteins due to its distinct advantages such as rapid growth rate, cost-effectiveness, many genetic tools, easy scale-up, and convenience for high-cell-density cultivation (HCDC) (Makino et al., 2011a). In this regard, the production of therapeutic proteins (e.g., antibodies, scaffold proteins, vaccines, enzymes, receptors) in *E. coli* has been increasingly attracting attention (Lee et al., 2005). Most therapeutic proteins require the correct formation of disulfide bonds for the desired biological activity; thus, the periplasm of *E. coli* has been chosen for the production of these proteins (de Marco, 2009, 2012). In addition, secretory production provides several benefits such as N-terminal authenticity by signal peptide cleavage, ease of purification during the downstream process, and less proteolysis (Lee et al., 2005; Yoon et al., 2010).

For the secretory production of recombinant proteins in *E. coli*, two different pathways passing through the membrane-associated SecYEG translocon are available (Beckwith, 2013). First, Sec pathway which derive the post-translational translocation of unfolded proteins through the SecYEG translocon is responsible for the secretion of the majority of *E. coli* secretory proteins. Although various therapeutic proteins are successfully secreted via the Sec pathway (Jeong and Lee, 2000; Makino et al., 2011b; Sockolosky and Szoka, 2013; Sonoda et al., 2011), the problem of cytoplasmic aggregation prior to translocation is frequently encountered (Georgiou and Segatori, 2005; Huang et al., 2012). Next, as an alternative secretion pathway, the signal recognition particle (SRP)-dependent pathway is gaining in interest. The SRP pathway shares the SecYEG translocon with the Sec pathway (Beckwith, 2013), but the cytoplasmic aggregation can be effectively prevented since the translocation coincidentally occurs during the protein synthesis (co-translational translocation) (Puertas et al., 2010). Thereby, the SRP pathway has been especially more useful for the production of easy-to-aggregate proteins such as the fast-folding proteins originated from unrelated organisms (Lee et al., 2013; Puertas et al., 2010; Steiner et al., 2006) or inner membrane proteins that have multiple transmembrane segments (Nannenga and Baneyx, 2011; Skretas et al., 2012). However, severe growth defects were reported occasionally when excess proteins were secreted via

Correspondence to: K.J. Jeong
Contract grant sponsor: Ministry of Science, ICT and Future Planning (MIFP)
Contract grant number: 2014M3A6A8066443
Received 18 December 2015; Revision received 7 April 2016; Accepted 21 April 2016
Accepted manuscript online 25 April 2016;
Article first published online 11 May 2016 in Wiley Online Library (http://onlinelibrary.wiley.com/doi/10.1002/bit.25997/abstract).
DOI 10.1002/bit.25997

the SRP pathway (Lee et al., 2013; Makino et al., 2011b). This phenomenon is thought to be caused by the insufficient capacity of the *E. coli* SRP pathway, as the Sec pathway possesses dominant portion of the SecYEG translocon-mediated protein secretion (Georgiou and Segatori, 2005). In order to solve this problem, several efforts such as controlling the endogenous level of SRP pathway-related biomolecules have been made. Until now, the co-expression of Ffh (protein component of SRP), 4.5S RNA (encoded by *ffs*, RNA component of SRP), or FtsY (SRP receptor) is known to be effective for SRP-dependent protein production (Lee et al., 2013; Nannenga and Baneyx, 2011; Puertas et al., 2010). In addition, it was discovered that knocking out Trigger Factor (TF, encoded by *tig*) could improve the SRP machinery, promoting the competitive binding of SRP to the ribosome (Nannenga and Baneyx, 2011; Puertas et al., 2010). Besides, co-expression of YidC, the inner membrane protein insertase, has a positive effect on SRP-dependent protein production (Lee and Jeong, 2013; Nannenga and Baneyx, 2011). In spite of various efforts, the application of the SRP pathway is still limited since the secretion capacity has been insufficient in many cases. In this regard, even more studies and techniques are required for the versatile use of the SRP pathway.

In this study, we sought to engineer *E. coli* towards the enhanced production of recombinant proteins via SRP-dependent secretory pathway. For this purpose, we first constructed transposon-inserted random library, and using a novel FACS-based screening system, the *E. coli* mutants exhibiting remarkably higher secretory production could be successfully isolated. In the engineered *E. coli* mutant, the enhanced capability of protein secretion via SRP-dependent pathway was also demonstrated with the various protein models including endogenous SRP-dependent proteins, recombinant antibodies and G protein-coupled receptor. Further, we performed fed-batch cultivations to produce the therapeutic proteins (i.e., IgG, GPCR) using the engineered *E. coli* mutant, and remarkably high production yield (gram-scale) was achieved compared to that observed in previous reports.

Materials and Methods

E. coli Strains and Plasmids Construction

All *E. coli* strains, plasmids (Table S1) and oligonucleotide primers (Table S2) used in this study are listed in supporting information. Oligonucleotide primers for molecular cloning and genomic analysis are also listed in supporting information (Table S2). *E. coli* MG1655 was used for gene cloning and all of the other experiment except IgG expression. To analyze the effect of isolated mutant (YJ001), deleterious knockout mutant (YJ002) was constructed by using "Rapid One-Step Inactivation" method (Song and Lee, 2013). The gene knockout was performed with the primer set of RrsE KO F/R. For the production of IgG, *E. coli* XL1-Blue was used, and YJ003 was also constructed for evaluating the effect of knockout. For the development and evaluation of periplasmic fluorescent reporter system, pMMBPF was constructed. Coding gene of *E. coli* maltose binding protein (MBP) was amplified from chromosomal DNA of *E. coli* MG1655 by using the primer set of MMBPF F and MBPF R. The amplified DNA fragment was digested with *Xba*I and *Hin*dIII restriction endonucleases, and then the digested fragment was ligated into the corresponding site of pMoPac16, yielding pMMBPF. Similarly, pMBPF and pDMBPF were constructed by using the primers of MBPF F or DMBPF F, respectively, instead of MMBPF F. Expression plasmids for endogenous SRP-dependent proteins were also constructed in similar way. The primer sets of DsbA F/R, TorT F/R, or TolB F/R were used for the construction of corresponding expression vectors, respectively. DsbA signal peptide-fused rat NTR1 D03 gene was synthesized by using commercial service (Mutagenex Inc., Suwanee, GA). The subcloned gene was digested and ligated into the *Xba*I-*Hin*dIII site of pMoPac16, yielding pDrNTR1. All genetic manipulations (e.g., restriction digestion, ligation, agarose gel electrophoresis) were conducted according to the standard procedures (Sambrook and Russell, 2001).

Library Screening

Randomly mutated *E. coli* library was prepared by using EZ-Tn5^{TM} <KAN-2> Tnp Transposome^{TM} kit (Epicentre, Madison, WI). After random mutagenesis, transposon-inserted mutants were transformed with pDMBPF to generate the final library for screening. The cells were inoculated in TB media at 37°C, and gene expression was induced at 25°C by adding 1 mM IPTG (final concentration). After further cultivation for 20 h, cells were harvested by centrifugation (6,000 rpm, 10 min, and 4°C), and the cell pellets were resuspended in 1× phosphate buffered saline (PBS) containing 25 μM of FlAsH (Santa Cruz Biotech, Inc., Dallas, TX) at room temperature for 90 min. Then, cells were washed twice with 1× PBS, and the high-throughput screening was performed by using MoFlo^{TM} XDP (Beckman Coulter, Inc., Brea, CA) equipped with 488 nm laser and 530/40 nm band pass filter. About 70% of cells were firstly selected based on the location in FSC-SSC plot (right-bottom side of main population), and then, among this population, 3% of cells having high fluorescence signal was finally sorted. The sorted cells were resorted without change of sorting gates, and the resorted cells were spread on LB-agar plate containing 50 mg/L of kanamycin and 100 mg/L ampicillin. After overnight cultivation, the cells grown on agar plate were scraped and subjected to the next round of sorting and resorting.

Genomic Analysis of the Isolated Mutant

Genomic DNA of *E. coli* strains was extracted by using MasterPure^{TM} Complete DNA and RNA Purification Kit (Epicentre). The purified genomic DNA was digested by using *Xba*I restriction endonuclease (Enzynomics), and then the small-sized fragments (<3 kb) were purified through agarose gel electrophoresis followed by band extraction. The digested DNA fragments were ligated and the gene was amplified by using the transposon specific primers, KAN-2 F and KAN-2 R (Table S2). The amplified genes were cloned into pJET1.2/blunt by using CloneJET PCR Cloning Kit (Thermo Fisher Scientific, Waltham, MA), and then the sequence was analyzed to identify the genetic feature of isolated mutants. Colony PCRs were performed to confirm the location of transposon disruption according to standard protocols (Sambrook and Russell, 2001), by using EmeraldAmp GT PCR Master Mix (Takara Bio Inc., Shiga, Japan).

Cytometric Analysis for Evaluating the Expression Level of Active NTR1 D03

Fluorescently labeled agonist [BODIPY-NT(8-13)] (Sarkar et al., 2008) was prepared by using commercial peptide synthesis service. After cultivation and protein expression, the cells were harvested, and then spheroplasting was performed as previously described (Jung et al., 2007). The prepared spheroplasts were resuspended in 1× PBS containing 5 μM of BODIPY-NT(8-13) and it was incubated in room temperature for 90 min with vigorous mixing. After fluorescent labeling, cytometric analysis was performed by using MoFlo^{TM} XDP (Beckman Coulter, Inc.) equipped with 488 nm laser and 530/40 nm band pass filter.

Flask Cultivations for Protein Expression

Cells were inoculated in liquid TB media (BD) containing 2% glucose and appropriate antibiotics (50 mg/L of kanamycin, 100 mg/L ampicillin, and/or 35 mg/L chloramphenicol). After overnight cultivation at 37°C, cells were transferred into 10 mL of fresh liquid TB media without glucose in 100 mL flasks, and then the cells were incubated at 37°C. When the cells reached to an OD_{600} of around 0.5, protein expression was induced by adding the appropriate inducers (1 mM of IPTG w/ or w/o 0.2% of L-arabinose), and cells were allowed to grow at 25°C for 16 h.

Fed-Batch Cultivation

YJ003 harboring pDLPH + pBAD33*ffh/dsbC* or YJ002 harboring pDrNTR1 + pBAD33*yidC* was adapted to R/2 minimal media by performing several subcultures until the cells were well grown in the media. After the media adaptation, the inoculum was prepared in 200 mL of R/2 minimal media containing 20 g/L of glucose, and it was subjected to the fed-batch cultivation. Detailed procedure of fed-batch cultivation was already described in the previous study (Lee et al., 2013). Expression of IgG and folding assistants were induced after reaching OD_{600} of around 60 at 25°C, by adding 1 mM IPTG and 0.2% L-arabinose. Small amount of culture solution was periodically harvested during the cultivation, and the samples were used for the analysis and quantification. Production yield of fully assembled IgG was quantified via enzyme-linked immunosorbent assay (ELISA) by using purified IgG as a standard. The yield of NTR1 D03 was quantified by using densitometry. Detailed procedures for ELISA and protein purification were previously described (Lee et al., 2013).

Analytical Methods

Procedures for SDS–PAGE analysis, Western blot analysis and RT-qPCR are described in supporting information.

Results and Discussion

PECS-FlAsH Assay for Evaluating Periplasmic Expression

For the cytometric isolation of SRP machinery-enhanced *E. coli* mutants, development of a fluorescent reporter system that can evaluate periplasmic expression is required. Thus, we designed a "PECS-FlAsH method" by combining periplasmic expression with cytometric screening (PECS) strategy (Chen et al., 2001) and fluorescein arsenical hairpin binder-ethanedithiol (FlAsH-EDT_2; more briefly, FlAsH)-mediated staining. FlAsH can specifically bind to the proteins that contain a tetracysteine motif (-CCXXCC-), and exhibit fluorescence only after the binding (Griffin et al., 2000). Thus, we expected the secreted proteins, which are fused to a tetracysteine motif, to be selectively labeled with FlAsH and the fluorescence intensities of cells to correlate with the periplasmic level of the target protein in the cells.

To demonstrate the concept of PECS-FlAsH method, we constructed two plasmids (pMBPF and pMMBPF), which express maltose-binding protein (MBP) in the cytoplasm or the periplasm, respectively (Fig. 1A). In both constructs, an optimized tetracysteine motif (-FLNCCPGCCMEP) was fused to C-terminus of MBP for the binding of FlAsH (Martin et al., 2005). To find the optimal condition for FIAsH labeling, two factors were tested: (i) concentration of the phosphate buffered saline (PBS); and (ii) concentration of FlAsH in the reaction buffer. First, the following four concentrations of PBS were examined: 0.7, 1, 2, and 5× PBS. After cultivation and FlAsH (25 μM) labeling, fluorescence intensity in each cell was analyzed by flow cytometry, and we found that the best result in which the fluorescence signals of the positive and negative controls were fully separated was obtained when the cells were mixed with FlAsH in 1× PBS. The cells harboring pMMBPF, which has the coding gene of periplasmically

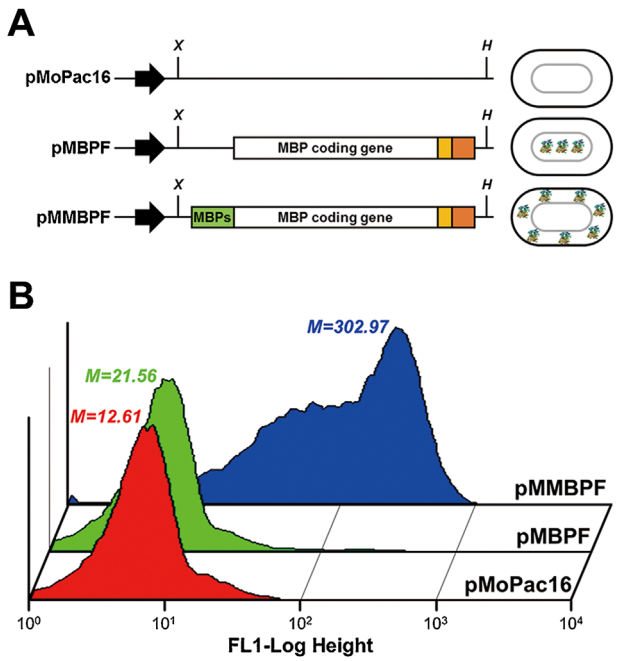

Figure 1. Development of FlAsH-based periplasmic fluorescent reporter system. (**A**) Plasmid structures and schematic diagram of protein expression and secretion. *X* and *H* represent *Xba*I and *Hin*dIII restriction enzyme site, respectively. (**B**) Cytometric analysis of FlAsH-labeled *E. coli* cells harboring model plasmids (pMoPac16, pMBPF, or pMMBPF). *X*-axis means fluorescence intensity through 520/30 bandpass filter. *M* values represent mean fluorescence intensity.

secreted MBP, exhibited much higher fluorescence intensity ($M = 302.97$) than those harboring pMBPF ($M = 21.56$) or pMoPac16 ($M = 12.61$) (negative controls) (Fig. 1B). On the other hand, we could not obtain the desired results in lower or higher concentrations of PBS (Fig. S1). Under the low-salt condition (0.7× PBS), all the cells exhibited low fluorescence signals due to poor permeability (Fig. S1A), and under the high-salt conditions (2 and 5× PBS), non-specific fluorescence signals were observed due to too high permeability (Fig. S1B and C). Next, we examined three different concentrations of FlAsH (5, 10, and 25 μM) in 1× PBS, and we got the best result with 25 μM of FlAsH. When the cells were labeled with smaller amounts of FlAsH (5 and 10 μM), fluorescence signals between negative (pMBPF and pMoPac16) and positive (pMMBPF) models were not fully separated (Fig. S1D and E). For our next experiments, we used this optimal condition (25 μM of FlAsH in 1× PBS) for FlAsH labeling.

Isolation of SRP Machinery-Enhanced *E. coli* Mutants by Screening of Random Library

To isolate the SRP machinery-enhanced mutants, the *E. coli* MG1655 mutant library was constructed using transposon (Tn5)-mediated random insertional knockout. More than 10^7 colonies were obtained. As a reporter system, a pDMBPF plasmid, which contains MBP fused to DsbA signal peptide, was constructed so that the MBP can be secreted into the periplasm via the SRP-dependent pathway. Then, the pDMBPF plasmid was transformed into the Tn5-mediated random library, and more than 10^8 colonies were successfully obtained. After cultivation, the cells were labeled with FlAsH under the optimized condition, and the highly fluorescent cells were selectively sorted by FACS. After the fourth round screening of the library, cells showing fairly increased fluorescence signals were found to be enriched (Fig. 2A). From the fourth round-sorted cells, five individual clones were randomly selected, and their MBP expression levels were compared with those of the wild-type MG1655. In SDS–PAGE analysis, all five of the isolated clones exhibited significant increase in MBP production compared with the wild-type MG1655 (Fig. 2B). In addition, secretion yields of MBP in the periplasm were significantly enhanced in the isolated clones (Fig. 2B). When compared with the wild-type MG1655, about 3.8-fold increase in the expression level and 3.1-fold increase in the secretion yield were determined by densitometric analysis.

Next, after curing the plasmids (pDMBPF) from the five isolated clones, cells were re-transformed with either pMMBPF (for Sec-dependent secretion using MBP's own signal peptide) or pDMBPF (for SRP-dependent secretion using DsbA signal peptide) to determine whether the isolated mutants were effective only for SRP-dependent protein secretion. After cultivation, production and secretion of MBP in each clone were analyzed by SDS–PAGE. Results showed that expression and secretion of MBP were increased again in all of the isolated mutants harboring pDMBPF compared to wild-type MG1655 (Fig. 3A). In contrast, all isolated mutants harboring pMMBPF showed similar production and secretion levels to the wild-type MG1655 (Fig. 3B). Additionally, unlike as secretion via SRP-dependent pathway, the premature forms, which were not secreted into the periplasm, were observed in all examined strains (Fig. 3B). Here, it was also experimentally demonstrated that the

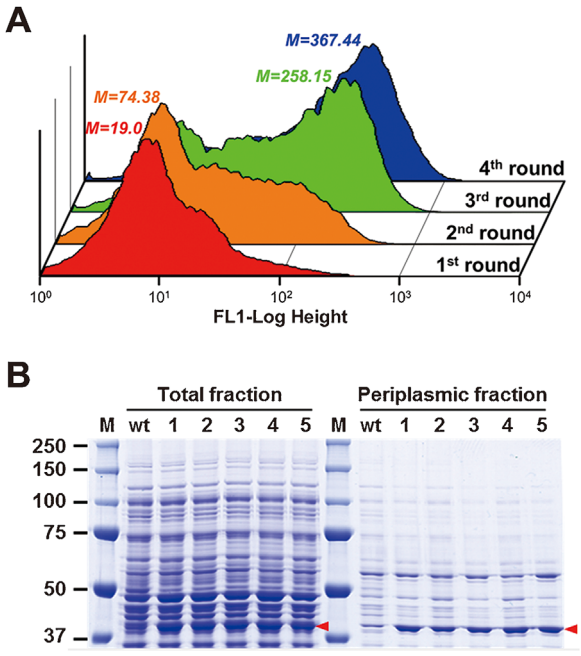

Figure 2. Isolation of SRP machinery-enhanced *E. coli* mutants via FACS. (**A**) Enrichment of fluorescence signal during the screening. Red, orange, green, and blue histograms represent 1st, 2nd, 3rd, and 4th round screening, respectively. *M* values represent mean fluorescence intensity. (**B**) SDS–PAGE analysis of MBP production in the isolated clones. Numbered lanes are five random individual clones.

accumulation of premature aggregates in the cytoplasm would be prevented by SRP pathway which mediates co-translational translocation as described in the introduction section. Interestingly, in wild-type MG1655, the production of MBP via SRP pathway showed much lower yield than that by Sec-pathway (Fig. 3A and B). The lower production yield in SRP pathway may be ascribed to relatively poorer expression of MBP gene with DsbA signal peptide (for SRP pathway) compared with MBP gene expression with its own signal peptide (for Sec pathway). In *E. coli*, the gene expression can be affected by several factors including TIR (Translation Initiation Region) (Lee et al., 2014; Seo et al., 2013). The DsbA signal peptide fused MBP may be unfavorable for transcription/translation. However it does not mean the DsbA signal peptide is not good for secretory production via SRP pathway. In the cases of other proteins including antibody fragments and full-length IgG, the use of same DsbA signal peptide did not cause the decreases of gene expression (Lee and Jeong, 2013; Lee et al., 2013). For the efficient gene expression, it is also important to choose the proper signal peptide for target proteins. Overall, the results suggest that all isolated mutants have enhanced secretion ability specifically for the SRP-dependent secretion pathway, while the same is not true for the Sec pathway.

Identification and Characterization of the Isolated Mutants

Genetic changes in five isolated mutants were investigated by the inverse PCR method (Ochman et al., 1988) followed by DNA

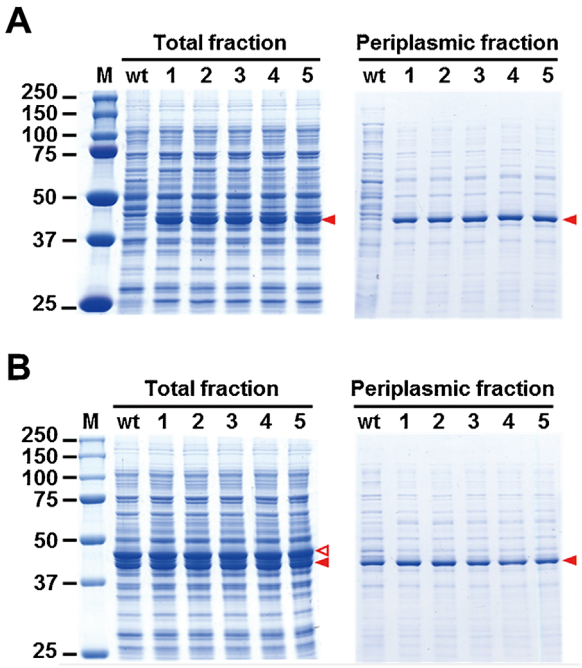

Figure 3. Comparison of SRP/Sec-dependent protein expression and secretion in the isolated clones. The isolated clones were transformed with (**A**) pDMBPF (for SRP pathway) and (**B**) pMMBPF (for Sec pathway), respectively. Then, the expression and secretion of MBP were analyzed by SDS–PAGE. Closed and open arrowheads represent the periplasmic (mature) MBP and cytoplasmic (premature) MBP, respectively.

sequencing, and the results clearly revealed that all of the isolated mutants had the same genetic change: interruption of 16S ribosomal RNA coding gene (*rrsX*) by transposon insertion (Fig. S2A). It is well-known that *E. coli* has seven copies of *rrsX* (i.e., *rrsA*, *rrsB*, *rrsC*, *rrsD*, *rrsE*, *rrsG*, *rrsH*) with very high homology (Weider et al., 2005), and further PCR analysis revealed that, *rrsE* among the seven *rrsX* genes was knocked out by transposon insertion (Fig. S2B). The isolated mutant with the transposon-mediated *rrsE* gene knock out was named YJ001.

Enhanced Expression and Secretion of Endogenous SRP-Dependent Secretory Proteins

To evaluate the effect of *rrsE* disruption on protein secretion via the SRP pathway, we generated an *rrsE*-deficient mutant (named YJ002) by using "Rapid One-Step Inactivation" method (Song and Lee, 2013). We first compared the growth of YJ002 strain with that of the parental MG1655 strain to determine whether the cell growth is affected by the deletion of *rrsE*. During the cultivation in flask, we could not find any differences in the growth of both strains (Fig. S3A). Next, the levels of MBP expression and secretion in *E. coli* YJ002 harboring pDMBPF were compared with those of the wild-type MG1655 and the isolated mutant (YJ001). In both YJ001 and YJ002, similar levels of expression and secretion were observed, which were much higher than those of the wild-type MG1655 (Fig. 4A). In addition, *E. coli* YJ002 harboring pDMBPF showed similar patterns of cell growth to wild-type MG1655 harboring the same plasmid during the protein production (Fig. S3B).

Next, we also examined the generic effect of *rrsE*-deficient strains on the secretion of three representative endogenous proteins (DsbA, TorT, and TolB), which have their own signal peptides and are secreted into the periplasm via the same SRP-dependent pathway. The genes coding for each protein were cloned into the expression vector (pMoPac16), yielding pDsbA, pTorT, and pTolB, respectively. After transformation into both the *rrsE*-deficient mutants, YJ001 and YJ002, the expression and secretion levels of each protein were compared with those in wild-type MG1655. In all cases, the expression of the proteins of interest (DsbA, TorT, and TolB) was increased in both the mutant strains (YJ001 and YJ002) compared to the wild-type, irrespective of the signal peptides used for secretion (Fig. 4B). As the expression level increased, the amount of secreted proteins of interest also increased. In addition to the expression in plasmid, we also examined the expression of

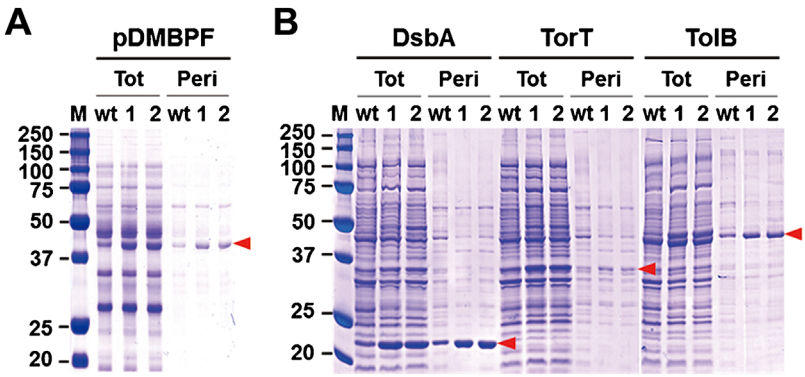

Figure 4. SDS–PAGE analysis of protein production in *rrsE*-deficient *E. coli* mutant. (**A**) MBP production in the wild-type and *rrsE*-deficient mutants harboring pDMBPF. (**B**) Expression and secretion of endogenous SRP-dependent proteins (DsbA, TorT, and TolB) in the wild-type and *rrsE*-deficient *E. coli* mutants. In all panels, lanes M, wt, 1 and 2 represent protein size marker, *E. coli* MG1655, *E. coli* YJ001, and *E. coli* YJ002, respectively. Tot and Peri indicate total and periplasmic fraction of protein extract, respectively. Closed arrowheads denote correctly expressed and secreted target proteins.

endogenous DsbA from chromosomal DNA of wild-type MG1655 and mutant YJ002. After cultivation, the level of DsbA in each cell was analyzed by western blotting, and we found that a little higher secretion yield of DsbA was also obtained in YJ002 strain compared to the wild-type MG1655 (Fig. S4). Overall, the data suggest that deletion of *rrsE* gene has a significant effect on protein secretion via the SRP-dependent pathway.

Enhanced Secretory Production of Antibodies in *rrsE*-Deficient Mutant

During the production of antibodies and antibody fragments in *E. coli*, they need to be secreted into the periplasm for the correct formation of disulfide bonds. In our previous study (Lee and Jeong, 2013), we have shown enhanced production of the antibody fragment M18 scFv against anthrax toxin PA via the SRP-dependent pathway in *E. coli* MG1655 (about 3.7-fold increase), and here we examined whether the use of *rrsE*-deficient *E. coli* strain is effective for the production of scFv. The plasmid, pDM18, in which M18 scFv was fused to DsbA signal peptide (Lee and Jeong, 2013), was transformed into both the wild-type MG1655 and *rrsE*-deficient YJ002, and the expression levels of M18 scFv were compared. Similar to the other model proteins, the expression level of M18 scFv was significantly increased (about 3.1-fold increase, 1.9 mg/L of scFv) in YJ002 (Fig. 5A), and more scFv was also detected in the periplasm of YJ002 than in the wild-type (Fig. 5A).

In addition to scFv, production of full-length IgG was also examined. In our previous study, we developed pDLPH plasmid for IgG production in *E. coli*, in which a light chain (L-chain) and a heavy chain (H-chain) are secreted via the SRP- and Sec-dependent pathway, respectively (Lee et al., 2013). In that study, the amount of full-length IgG produced was as high as 62 mg/L by fed-batch cultivation of *E. coli* XL1-Blue, which was chosen from strain test, harboring pDLPH and pBAD33*ffh/dsbC* (for co-expression of *ffh* and *dsbC* genes). Here, to examine the effect of *rrsE* deletion on IgG production, we developed *rrsE*-deficient *E. coli* XL1-Blue (named YJ003), and subsequently pDLPH and pBAD33*ffh/dsbC* plasmids were co-transformed into *E. coli* YJ003. After flask cultivation, the secretion and production yields of IgG were compared with those of the wild-type XL1-Blue. *E. coli* YJ003 showed increased expression of the light chain which was secreted via the SRP pathway, whereas the expression of heavy chain via the Sec-dependent pathway was

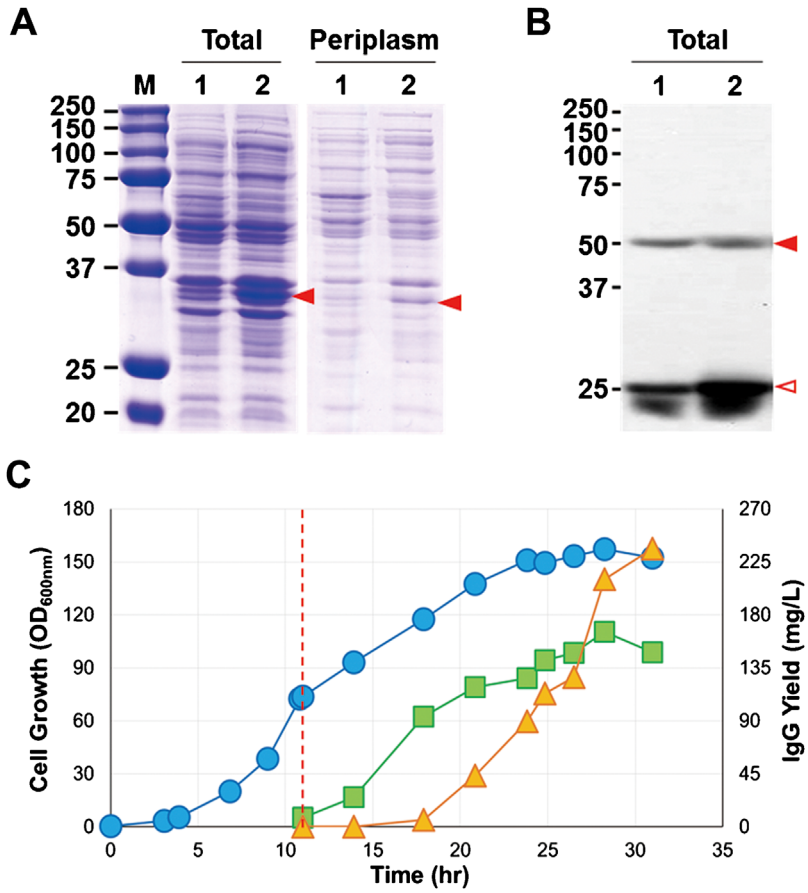

Figure 5. Production of antibodies (scFv and full-length IgG) in *rrsE*-deficient mutants. (**A**) SDS–PAGE analysis of production of M18 scFv. Lanes 1 and 2 represent *E. coli* MG1655 and *E. coli* YJ002, respectively. Closed arrowheads indicate M18 scFv. (**B**) Western blot analysis of IgG production in flask cultivation. Lanes 1 and 2 represent *E. coli* XL1-Blue and *E. coli* YJ003. Open and closed arrowheads represent light and heavy chains of IgG, respectively. (**C**) Time profiles of cell growth and IgG production in the fed-batch cultivation. The dashed line indicates the time point of IPTG induction. Symbols: Circle (●), cell density (OD_{600}); Square (■), yield of periplasmic IgG (mg/L); Triangle (△), yield of extracellular IgG (mg/L).

not changed compared to that in the wild-type XL1-Blue strain (Fig. 5B). Next, we performed fed-batch cultivation to examine the large-scale production of IgG in *E. coli* YJ003. After cultivation, the amount of fully assembled IgG in the periplasm was quantified by ELISA. When cultured for 31 h, the maximum production yield of 165.4 mg/L was achieved, which was about 2.7-fold higher than that obtained previously (~62 mg/L) with wild-type *E. coli* XL1-Blue (Lee et al., 2013) (Figs. 5C and S5A). The maximum volumetric productivity was 5.85 mg/L/h, which was also 2.6-fold higher than that obtained with the wild-type strain (2.21 mg/L/h) (Fig. 5C; Table S3). In addition to the periplasmic level of the antibody, we also looked for an extracellular titer of IgG because the leakage of periplasmic proteins into the culture supernatant was occasionally reported (Puertas et al., 2010). Surprisingly, it was observed that significant amount of IgG (236.5 mg/L) was accumulated in the extracellular medium (Figs. 5C and S5B). The cause of this accumulation could not be the cell lysis during cultivation because cell density continued to increase during the accumulation of IgG in the extracellular medium (Fig. 5C). The cell specific growth rate ($\mu = 0.044\ h^{-1}$) and maximum cell density (OD_{600} of 157.2) in this fed-batch cultivation was similar to those in the previous fed-batch cultivation with *E. coli* XL1-Blue, although no accumulation of IgG in the extracellular medium was observed in the previous culture. In the present fermentation, 384.7 mg/L of full-length IgG could be produced in total and the volumetric productivity was about 13 mg/L/h, which was almost sixfold higher than the wild-type XL1-Blue (2.21 mg/L/h) (Table S3).

Production of G Protein-Coupled Receptor in *rrsE*-Deficient Strain

The rat neurotensin receptor 1 (NTR1) D03 mutant is a well-known G protein-coupled receptor (GPCR) variant, which has neurotensin binding activity (Sarkar et al., 2008). The correct cellular location of *E. coli*-driven GPCR is the inner membrane; thus, the secretion and integration of NTR1 D03 would be mediated by the SRP-dependent pathway (Puertas et al., 2010; Skretas et al., 2012). For this reason, we expected the expression and membrane integration of NTR1 D03 to be increased in the *rrsE*-deficient strain. A gene encoding rat NTR1 D03 mutant was synthesized and cloned into the expression vector (pMoPac16), yielding pDrNTR1, and *E. coli* MG1655 and YJ002 were co-transformed with pDrNTR1 and pBAD33*yidC*, respectively. Here, pBAD33*yidC*, which is the inner membrane protein insertase (YidC)-expressing plasmid (Lee and Jeong, 2013), was employed to further enhance the secretion and integration of NTR1 D03. After cultivation, the cells were labeled with the fluorescent ligand [BODIPY-NT(8-13)] of NTR1 D03 (Sarkar et al., 2008), and cytometric analysis was performed to analyze the expression and binding activity of NTR1 D03 in the inner membrane of each strain. When the cells were induced by IPTG, *E. coli* YJ002 exhibited about 2.5-fold higher fluorescence intensity than the wild-type (Fig. 6A). This result indicates the higher level of active NTR1 D03 in the inner membrane of *E. coli* YJ002 than in the wild-type *E. coli* MG1655. Using purified NTR1 D03 as a standard, the level of NTR1 D03 in YJ002 strain was densitometrically quantified as 20.9 mg/L (Fig. S6). This was a

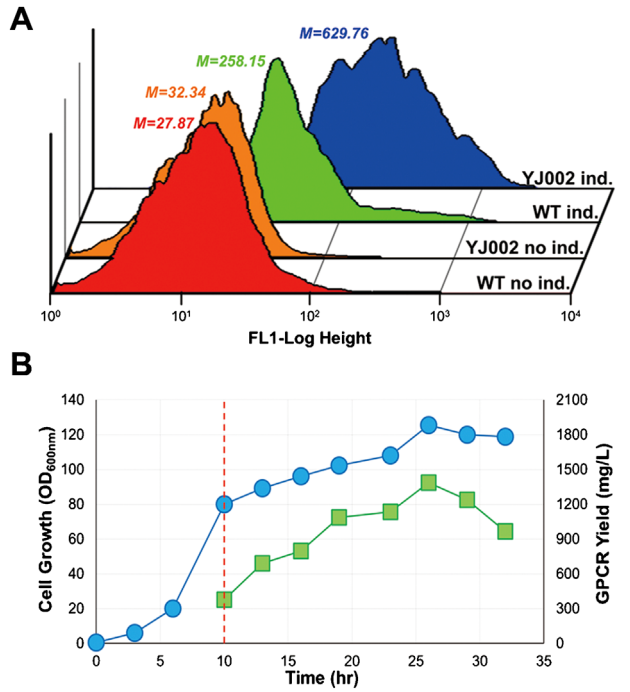

Figure 6. Production of G protein-coupled receptor (NTR1 D03) in *rrsE*-deficient mutants. (**A**) Cytometric analysis of NTR1 D03 production in wild-type MG1655 and YJ002. "ind." and "no ind." represent the cells w/ or w/o IPTG induction, respectively. *X*-axis means fluorescence intensity through 520/30 bandpass filter. *M* values represent mean fluorescence intensity. (**B**) Time profiles of cell growth and NTR1 D03 production in the fed-batch cultivation. The dashed line indicates the time point of IPTG induction. Symbols: Circle (●), cell density (OD_{600}); Square (■), yield of NTR1 D03 (mg/L).

much higher value than the other reported production yields of GPCR in *E. coli* (0.5–8 mg/L) (Link et al., 2008; Sarkar et al., 2008). For the large-scale production of NTR1 D03, fed-batch cultivation was also carried out with *E. coli* YJ002 harboring pDrNTR1 and pBAD33*yidC*. In the fed-batch cultivation, high cell density (OD_{600} of 125.6) and production yield as high as 1.4 g/L could be achieved (Fig. 6B). When compared to previous studies, this was the most successful case of high cell density cultivation for GPCR production in *E. coli* (Milic and Veprintsev, 2015).

In-Depth Study on the Cellular Mechanism of *rrsE*-Deficient Mutant

Because the knocked out gene (*rrsE*) is a copy of 16S ribosomal RNA coding gene, we compared the ratio of 16S–23S rRNA in *rrsE*-deficient YJ002 and wild-type MG1655. After the preparation of total RNAs, we analyzed the samples by performing agarose gel electrophoresis and RT-qPCR. In both experiments, we observed that the ratio of rRNA did not change in YJ002, although the single copy of 16S rRNA coding gene (*rrsE*) was knocked out (Fig. 7A and B). Here, we assumed that a repair mechanism might be compensating for the loss of the 16S rRNA coding gene, so that the normal cellular levels of rRNA could be maintained. In addition, we also analyzed the transcript levels of *ffs* and *ffh* by RT-qPCR. Both 4.5S RNA (encoded by *ffs*) and Ffh are the component of SRP and it is known that

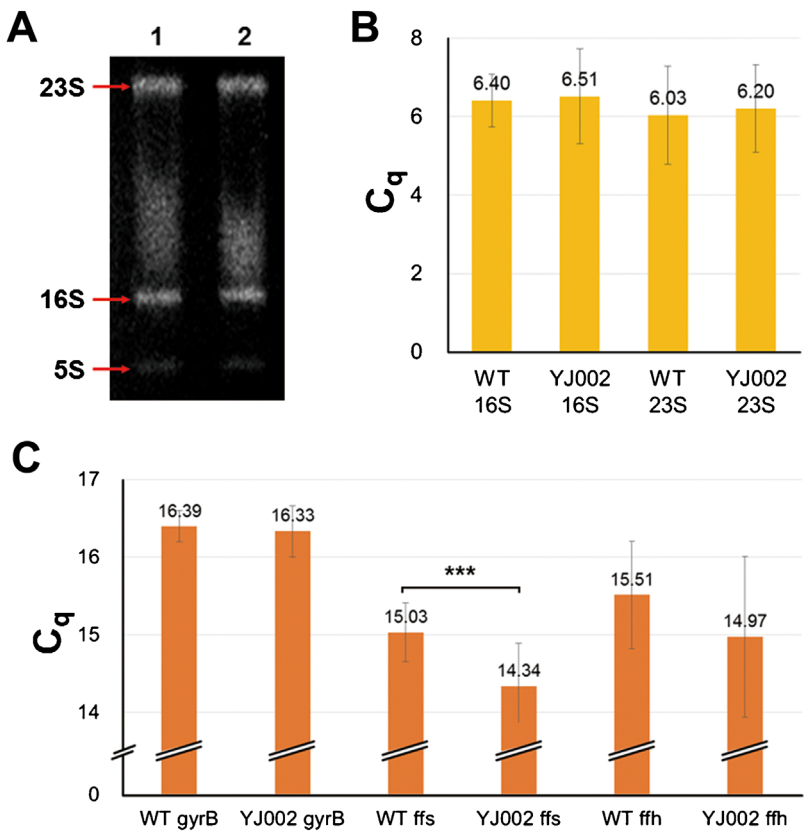

Figure 7. In-depth analysis of effect of *rrsE* deletion on protein secretion via SRP pathway. (**A**) Agarose gel electrophoresis for analyzing the rRNA contents in total RNA extracts. Lanes 1 and 2 represent MG1655 and YJ002, respectively. (**B** and **C**) C_q values from the RT-qPCR. (**B**) Comparison of the rRNA levels in wild-type *E. coli* MG1655 and YJ002. (**C**) Comparison of the transcript levels of SRP components (*ffs* and *ffh*) in wild-type and *rrsE*-deficient mutant. As an internal standard, transcript level of housekeeping gene (*gyrB*) was also compared. $^{***}P < 0.01$ (paired two-tailed *t*-test). *P* values for each experimental set were listed in supporting information (Table S4).

co-expression of the both genes allows the enhanced protein expression and secretion via the SRP-dependent pathway (Lee et al., 2013; Nannenga and Baneyx, 2011; Puertas et al., 2010). As a result, we confirmed that the transcript levels of both SRP components (*ffs* and *ffh*) increased (1.6- and 1.5-fold, respectively) in the mutant, whereas the level of *gyrB* (housekeeping gene as a negative control) did not change (Fig. 7C). From this result, we inferred that the level of SRP pathway-related biomolecules would be harmonically changed to the direction for improving the SRP pathway under the deletion of *rrsE* gene. However, rRNA transcription and SRP-dependent protein secretion are controlled by complex and intricate processes (Bibi, 2012; Dennis et al., 2004). Furthermore, the molecular mechanism of the SRP pathway has not yet been fully understood and most of the prevailing theories are only based on in vitro experiments (Bibi, 2012; Herskovits and Bibi, 2000). Thus, to understand the positive regulation of the SRP-dependent secretion machinery in *rrsX*-deficient strains, further extensive studies such as tracking the cellular level of numerous factors (e.g., FIS protein, σ factors, NTP, ppGpp) are required. Although the relationship between the rRNA knockout and SRP pathway could not be thoroughly revealed in this study, we believe that the results described above will provide important clues for revealing the mechanism of improved secretion via the SRP pathway.

Conclusion

In this work, using a novel screening system, we showed that SRP-dependent secretion could be significantly enhanced by the deletion of 16s ribosomal RNA coding gene (*rrsE*) in *E. coli*. Using various recombinant protein models including endogenous proteins, antibodies, and GPCR, we successfully demonstrated the enhanced production of recombinant proteins in the engineered *E. coli* strains. According to our results, deletion of the *rrsE* gene was not effective on Sec pathway but highly effective on SRP-dependent pathway. In addition, we found that the effect of *rrsE* deletion on SRP-dependent secretion was not limited to specific strains as well as signal peptides, and generally applied to various *E. coli* strains and various SRP-dependent signal peptides. Growth retardation problem, which was one of the major obstacles in the use of SRP-dependent secretion pathway, was not observed in *rrsE*-deficient *E. coli*, and significant amount of cell growth (particularly in the fed-batch cultivation) could be achieved with high productivity. In the case of rat NTR1 D03 protein production, we could achieve very high yield over than gram-scale, and to the best of our knowledge, this is the first successful report of GPCR production in *E. coli* using high-cell-density cultivation. The exact mechanism of the positive effect of *rrsE* gene deletion on SRP-dependent secretion needs to be

further investigated, as it will also be helpful to understand the mechanism of SRP-dependent secretion pathway in bacterial host. Due to its distinctive characteristic (co-translational translocation), SRP-dependent pathway can be more useful for the production of bigger and complex proteins such as full-length IgG, GPCR etc., and we believe that our strategy of SRP-dependent secretion in *rrsE*-deficient strain seems to be a widely applicable method to expand the range of protein production in *E. coli*.

This work was supported by the Intelligent Synthetic Biology Center of Global Frontier Project (Grant no. 2014M3A6A8066443) funded by the Ministry of Science, ICT and Future Planning (MSIP).

References

Beckwith J. 2013. The Sec-dependent pathway. Res Microbiol 164(6):497–504.

Bibi E. 2012. Is there a twist in the *Escherichia coli* signal recognition particle pathway? Trends Biochem Sci 37(1):1–6.

Chen G, Hayhurst A, Thomas JG, Harvey BR, Iverson BL, Georgiou G. 2001. Isolation of high-affinity ligand-binding proteins by periplasmic expression with cytometric screening (PECS). Nat Biotechnol 19(6):537–542.

de Marco A. 2009. Strategies for successful recombinant expression of disulfide bond-dependent proteins in *Escherichia coli*. Microb Cell Fact 8:26.

de Marco A. 2012. Recent contributions in the field of the recombinant expression of disulfide bonded proteins in bacteria. Microb Cell Fact 11:129.

Dennis PP, Ehrenberg M, Bremer H. 2004. Control of rRNA synthesis in *Escherichia coli*: A systems biology approach. Microbiol Mol Biol Rev 68(4):639–668.

Georgiou G, Segatori L. 2005. Preparative expression of secreted proteins in bacteria: Status report and future prospects. Curr Opin Biotechnol 16(5):538–545.

Griffin BA, Adams SR, Jones J, Tsien RY. 2000. Fluorescent labeling of recombinant proteins in living cells with FlAsH. Methods Enzymol 327:565–578.

Herskovits AA, Bibi E. 2000. Association of *Escherichia coli* ribosomes with the inner membrane requires the signal recognition particle receptor but is independent of the signal recognition particle. Proc Natl Acad Sci USA 97(9):4621–4626.

Huang CJ, Lin H, Yang X. 2012. Industrial production of recombinant therapeutics in *Escherichia coli* and its recent advancements. J Ind Microbiol Biotechnol 39(3):383–399.

Jeong KJ, Lee SY. 2000. Secretory production of human leptin in *Escherichia coli*. Biotechnol Bioeng 67(4):398–407.

Jung ST, Jeong KJ, Iverson BL, Georgiou G. 2007. Binding and enrichment of *Escherichia coli* spheroplasts expressing inner membrane tethered scFv antibodies on surface immobilized antigens. Biotechnol Bioeng 98(1):39–47.

Lee SY, Choi JH, Lee SJ. 2005. Secretory production of therapeutic proteins in *Escherichia coli*. Methods Mol Biol 308:31–42.

Lee YJ, Jeong KJ. 2013. Enhanced production of antibody fragment via SRP pathway engineering in *Escherichia coli*. Biotechnol Bioproc Eng 18(4):751–758.

Lee YJ, Lee DH, Jeong KJ. 2014. Enhanced production of human full-length immunoglobulin G1 in the periplasm of *Escherichai coli*. Appl Microbiol Biotechnol 98:1237–1246.

Lee YJ, Kim HS, Ryu AJ, Jeong KJ. 2013. Enhanced production of full-length immunoglobulin G via the signal recognition particle (SRP)-dependent pathway in *Escherichia coli*. J Biotechnol 165(2):102–108.

Link AJ, Skretas G, Strauch EM, Chari NS, Georgiou G. 2008. Efficient production of membrane-integrated and detergent-soluble G protein-coupled receptors in *Escherichia coli*. Protein Sci 17(10):1857–1863.

Makino T, Skretas G, Georgiou G. 2011a. Strain engineering for improved expression of recombinant proteins in bacteria. Microb Cell Fact 10:32.

Makino T, Skretas G, Kang TH, Georgiou G. 2011b. Comprehensive engineering of *Escherichia coli* for enhanced expression of IgG antibodies. Metab Eng 13(2):241–251.

Martin BR, Giepmans BN, Adams SR, Tsien RY. 2005. Mammalian cell-based optimization of the biarsenical-binding tetracysteine motif for improved fluorescence and affinity. Nat Biotechnol 23(10):1308–1314.

Milic D, Veprintsev DB. 2015. Large-scale production and protein engineering of G protein-coupled receptors for structural studies. Front Pharmacol 6:66.

Nannenga BL, Baneyx F. 2011. Reprogramming chaperone pathways to improve membrane protein expression in *Escherichia coli*. Protein Sci 20(8):1411–1420.

Ochman H, Gerber AS, Hartl DL. 1988. Genetic applications of an inverse polymerase chain reaction. Genetics 120(3):621–623.

Puertas JM, Nannenga BL, Dornfeld KT, Betton JM, Baneyx F. 2010. Enhancing the secretory yields of leech carboxypeptidase inhibitor in Escherichia coli: Influence of trigger factor and signal recognition particle. Protein Expr Purif 74(1):122–128.

Sambrook J, Russell DW. 2001. Molecular cloning: A laboratory manual. Cold Spring Harbor, NY, USA: Cold Spring Harbor Laboratory Press.

Sarkar CA, Dodevski I, Kenig M, Dudli S, Mohr A, Hermans E, Pluckthun A. 2008. Directed evolution of a G protein-coupled receptor for expression, stability, and binding selectivity. Proc Natl Acad Sci USA 105(39):14808–14813.

Seo SW, Yang JS, Kim I, Yang J, Min BE, Kim S, Jung GY. 2013. Predictive design of mRNA translation initiation region to control prokaryotic translation efficiency. Metab Eng 15:67–74.

Skretas G, Makino T, Varadarajan N, Pogson M, Georgiou G. 2012. Multi-copy genes that enhance the yield of mammalian G protein-coupled receptors in *Escherichia coli*. Metab Eng 14(5):591–602.

Sockolosky JT, Szoka FC. 2013. Periplasmic production via the pET expression system of soluble, bioactive human growth hormone. Protein Expr Purif 87(2): 129–135.

Song CW, Lee SY. 2013. Rapid one-step inactivation of single or multiple genes in *Escherichia coli*. Biotechnol J 8(7):776–784.

Sonoda H, Kumada Y, Katsuda T, Yamaji H. 2011. Effects of cytoplasmic and periplasmic chaperones on secretory production of single-chain Fv antibody in *Escherichia coli*. J Biosci Bioeng 111(4):465–470.

Steiner D, Forrer P, Stumpp MT, Pluckthun A. 2006. Signal sequences directing cotranslational translocation expand the range of proteins amenable to phage display. Nat Biotechnol 24(7):823–831.

Weider LJ, Elser JJ, Crease TJ, Mateos M, Cotner JB, Markow TA. 2005. The functional significance of ribosomal (r) DNA variation: Impacts on the evolutionary ecology of organisms. Ann Rev Ecol Evol Syst 36:219–242.

Yoon SH, Kim SK, Kim JF. 2010. Secretory production of recombinant proteins in *Escherichia coli*. Recent Pat Biotechnol 4(1):23–29.

Supporting Information

Additional supporting information may be found in the online version of this article at the publisher's web-site.